

# Single Higgs boson production at a photon-photon collider: a 2HDM/MSSM comparison

*David López-Val*<sup>1</sup>

*Institut für Theoretische Physik, Universität Heidelberg*

*Philosophenweg 16, D-69120 Heidelberg, Germany*

lopez@thphys.uni-heidelberg.de

**Abstract** We consider the loop-induced production of a single Higgs boson from direct  $\gamma\gamma$ -scattering at a photon collider. A dedicated analysis of the total cross section  $\langle \sigma_{\gamma\gamma \rightarrow h} \rangle$  (for  $h = h^0, H^0, A^0$ ), and the relative strength of the effective  $h\gamma\gamma$  coupling  $r \equiv g_{\gamma\gamma h}/g_{\gamma\gamma H_{SM}}$ , is carried out within the general Two-Higgs-Doublet Model (2HDM) and the Minimal Supersymmetric Standard Model (MSSM). We systematically survey representative regions over the parameter space, in full agreement with brought-to-date theoretical and phenomenological restrictions, and obtain production rates up to  $10^4$  Higgs boson events per  $500\text{fb}^{-1}$  of integrated luminosity. We identify trademark phenomenological profiles for the different  $\gamma\gamma \rightarrow h$  channels and trace them back to the distinctive dynamical features characterizing each of these models – most significantly, the enhancement potential of the Higgs self-interactions in the general 2HDM. The upshot of our results illustrates the possibilities of  $\gamma\gamma$ -physics and emphasizes the relevance of linear colliders for the Higgs boson research program.

## 1 Introduction

The LHC is now truly laying siege to the Higgs boson. The diphoton and gauge boson pair excesses recently reported by ATLAS and CMS [1] may indeed constitute, if confirmed, a first solid trace of its existence. In the meantime, the currently available data keeps narrowing down the mass range and the phenomenological portray under which the Higgs boson may manifest. On the other hand, strong theoretical motivation supports of the idea that Electroweak Symmetry Breaking (EWSB) is realized by some mechanism beyond that of the Standard Model (SM), viz. of a single, fundamental spinless field. One canonical example of the latter is the general 2HDM [2]. Here, the addition of a second scalar  $SU_L(2)$  doublet tailors a rich and disclosing phenomenology [3]. The 2HDM can be fully set along in terms of the the physical Higgs boson masses; the ratio  $\tan\beta \equiv \langle H_2^0 \rangle / \langle H_1^0 \rangle$  of the two Vacuum Expectation Values (VEVs)

<sup>1</sup>Presented at Linear Collider 2011: Understanding QCD at Linear Colliders in searching for old and new physics, 12-16 September 2011, ECT\*, Trento, Italy

giving masses to the up- and down-like quarks; the mixing angle  $\alpha$  between the two  $CP$ -even states,  $h^0, H^0$ ; and, finally, one genuine Higgs boson self-coupling, which we shall denote  $\lambda_5$ . The Higgs sector of the MSSM corresponds to a particular (supersymmetric) realization of the general (unconstrained) 2HDM [4]. For further details we refer the reader to Ref. [5], where all the notation, model setup and restrictions are discussed at length.

Following the eventual discovery of the Higgs boson(s) at the LHC, of crucial importance will be to address the precise experimental determination of its quantum numbers, mass spectrum and couplings to other particles. A linear collider (linac) can play a central role in this enterprise [6]. Dedicated studies have exhaustively sought for the phenomenological imprints of the basic 2HDM Higgs boson production modes, such as e.g. i) triple Higgs,  $e^+e^- \rightarrow 3h$  [7]; ii) inclusive Higgs-pair through EW gauge boson fusion,  $e^+e^- \rightarrow V^*V^* \rightarrow 2h+X$  [8]; iii) exclusive Higgs-pair  $e^+e^- \rightarrow 2h$  [5,9]; and iv) associated Higgs/gauge boson  $e^+e^- \rightarrow hV$  [10], with  $h \equiv h^0, A^0, H^0, H^\pm$  and  $V \equiv Z^0, W^\pm$ <sup>2</sup>. As a common highlight, all these studies report sizable production rates and large quantum effects, arising from the potentially enhanced Higgs self-interactions. These self-couplings, unlike their MSSM analogues, are not anchored by the gauge symmetry, and may thus be strengthened as much as allowed by the unitarity bounds. Interestingly enough, Higgs boson searches at an  $e^+e^-$  collider may benefit from alternative operation modes, particularly from  $\gamma\gamma$  scattering. In this vein, single ( $\gamma\gamma \rightarrow h$ ) and double ( $\gamma\gamma \rightarrow 2h$ ) Higgs boson pair production are examples of  $\gamma\gamma$ -induced processes which entirely operate at the quantum level. The effective (loop-mediated) Higgs/photon interaction  $g_{\gamma\gamma h}$  can be regarded as a direct probe of non-standard (charged) degrees of freedom coupled to the Higgs sector. The aforementioned single Higgs channels have been considered in the framework of the SM [12], the 2HDM [13] and the MSSM [14,15] and are known to exhibit excellent experimental prospects, not only due to the clean environment inherent to a linac machine, but also owing to the high attainable  $\gamma\gamma$  luminosity, and the possibility to tune the  $\gamma$ -beam polarization as a strategy to enlarge the signal-versus-background ratios<sup>3</sup>.

## 2 Numerical analysis

### 2.1 Computational setup

In this contribution we present a fully updated analysis of the process  $\gamma\gamma \rightarrow h$  ( $h = h^0, H^0, A^0$ ) and undertake a comparison of the 2HDM – versus the MSSM results. We focus our attention on the following two quantities: **i)** the total, spin-averaged cross section,

$$\langle\sigma_{\gamma\gamma\rightarrow h}\rangle(s) = \sum_{\{ij\}} \int_0^1 d\tau \frac{d\mathcal{L}_{ij}^{ee}}{d\tau} \hat{\sigma}_{\eta_i\eta_j}(\hat{s}), \quad (1)$$

---

<sup>2</sup>For related work in the context of MSSM Higgs boson production see e.g. [11].

<sup>3</sup>Analogous studies for the  $\gamma\gamma \rightarrow hh$  mode are available e.g. in Ref. [16].

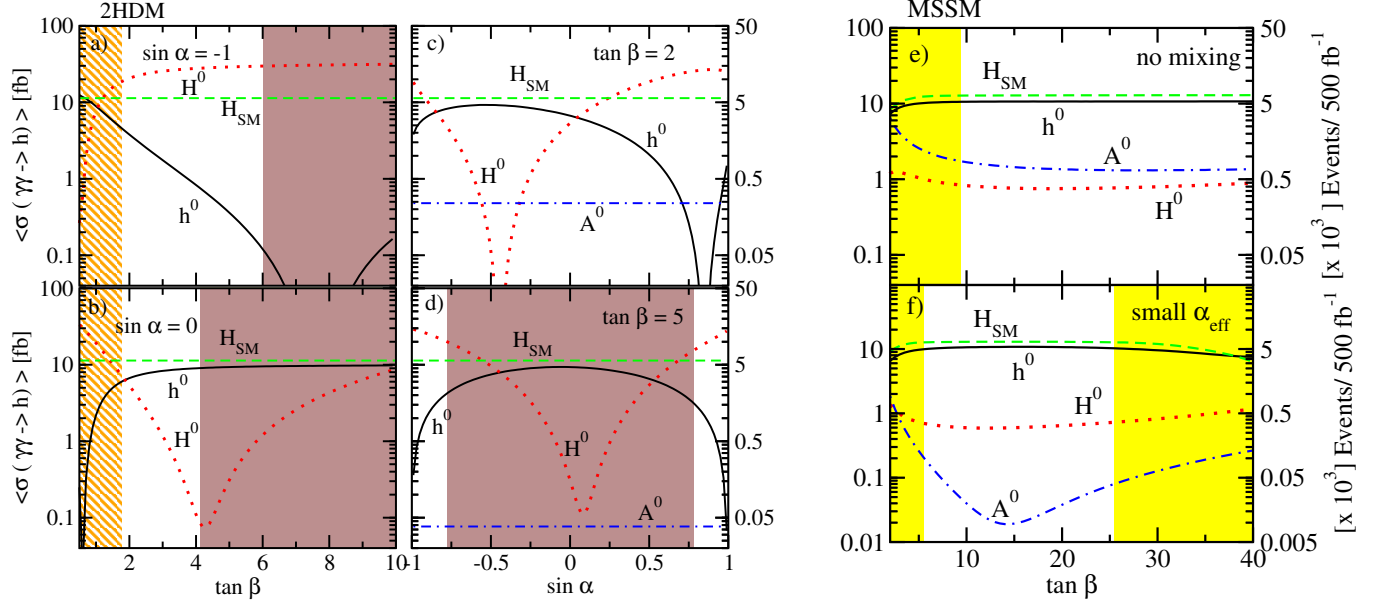


Figure 1: **Left panels (a-d):** Total spin-averaged cross-section  $\langle \sigma_{\gamma\gamma \rightarrow h} \rangle(s)$  and number of Higgs boson events, as a function of  $\tan \beta$  (a,b) and  $\sin \alpha$  (c,d) within the 2HDM. The shaded (resp. dashed) areas are excluded by unitarity (resp.  $B_d^0 - \bar{B}_d^0$  mixing). The Higgs boson masses are fixed as follows:  $M_{h^0} = 115 \text{ GeV}$ ;  $M_{H^0} = 165 \text{ GeV}$ ;  $M_{A^0} = 100 \text{ GeV}$ ;  $M_{H^\pm} = 105 \text{ GeV}$ , with  $\lambda_5 = 0$ . **Right panels (e-f):**  $\langle \sigma_{\gamma\gamma \rightarrow h} \rangle(s)$  within the MSSM, as a function of  $\tan \beta$ , for both the *no-mixing* and the *small- $\alpha_{eff}$*  benchmark points [17]. The dashed regions are ruled out by  $b \rightarrow s\gamma$  data. The linac center-of-mass energy is kept at  $\sqrt{s} = 500 \text{ GeV}$ .

where  $\hat{\sigma}_{\eta_i \eta_j}$  stands for the “hard” scattering cross section,  $\hat{s} = \tau s$  being the partonic center-of-mass energy; while  $d\mathcal{L}_{ij}^{ee}/d\tau$  denotes the (differential) photon luminosity distributions, by which we describe the effective  $e^\pm \rightarrow \gamma$  conversion of the primary linac beam. In turn,  $\eta_{i,j}$  accounts for the respective polarization of the resulting photon beams; and **ii)** the  $\gamma\gamma h$  coupling strength,  $r \equiv g_{\gamma\gamma h}/g_{\gamma\gamma H_{SM}}$  – that we normalize to the SM, identifying  $h^0 \equiv H_{SM}$ . We compare the distinct phenomenological patterns that emerge from the 2HDM and the MSSM and spell out the specific dynamical features that may help to disentangle both models. Further details may be found in Refs. [13, 14].

Throughout our study we make use of the standard algebraic and numerical packages FEYNARTS, FORMCALC and LOOPTOOLS [18]. Updated experimental constraints (stemming from the EW precision data, low-energy flavor-physics and the Higgs mass regions ruled out by the LEP, Tevatron and LHC direct searches), as well as the theoretical consistency conditions (to wit: perturbativity, unitarity and vacuum stability) are duly taken into account – cf. [19–24]. The photon luminosity distributions are obtained from [25], while the MSSM Higgs mass spectrum is provided by FEYNHIGGS [26].

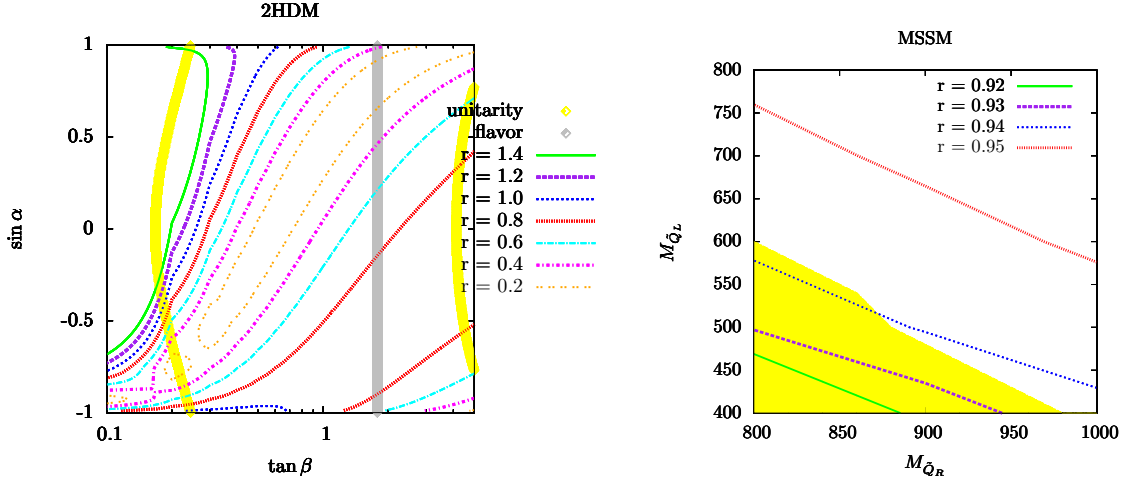


Figure 2: Contour plots of the ratio  $r \equiv g_{\gamma\gamma h^0}/g_{\gamma\gamma H_{SM}}$  that measures the effective  $\gamma\gamma h^0$  coupling strength normalized to the SM, for representative parameter space configurations, comparing the 2HDM (left panel) and MSSM (right panel). The 2HDM calculation is carried out assuming type-I Higgs/fermion Yukawa couplings,  $\lambda_5 = 0$  and the same set of Higgs boson masses as in Fig. 1. The yellow strips on the left plot denote the lower and upper bounds ensuing from unitarity, while the grey vertical band displays the restrictions stemming from  $B_d^0 - \bar{B}_d^0$ . As for the MSSM parameter setup, we employ  $\tan \beta = 2$ ,  $M_{A^0} = 600$  GeV,  $\mu = 500$  GeV,  $A_t = 1800$  GeV,  $M_2 = 500$  GeV. The dashed area is ruled out by  $b \rightarrow s\gamma$ . The linac center-of-mass energy is kept at  $\sqrt{s} = 500$  GeV.

## 2.2 Profiling $\gamma\gamma \rightarrow h$ within the 2HDM

The upshot of our numerical analysis is displayed on the left panels of Figs. 1 - 2. There we illustrate the behavior of  $\langle \sigma_{\gamma\gamma \rightarrow h} \rangle$  and the ratio  $r$  over representative regions of the 2HDM parameter space. For definiteness, we perform our calculation for a type-I 2HDM structure and for relatively light Higgs boson masses (as quoted in the Figure caption). The pinpointed trends, however, do not critically depend on the previous assumptions – see Ref. [13,14] for an extended discussion. Our results neatly illustrate the interplay of the charged Higgs boson,  $W^\pm$  boson and fermion loops, whose respective contributions to  $g_{\gamma\gamma h}$  undergo a highly characteristic destructive interference. The strength of the Higgs self-coupling  $\lambda_{hH^+H^-}$ , which is primarily modulated by  $\tan \beta$  and  $\lambda_5$ , determines whether the overall rates may become enhanced ( $r > 1$ ) or suppressed ( $r < 1$ ) relatively to the SM expectations. Scenarios yielding  $r > 1$  could in principle be met for  $\lambda_{hH^+H^-} \sim \mathcal{O}(10^3)$  GeV and  $M_{H^\pm} \sim \mathcal{O}(100)$  GeV (due to strongly boosted  $H^\pm$ -mediated loops) or  $\tan \beta < 1$  (which enhances the top-mediated loops through the Higgs-top Yukawa coupling,  $g_{h^0 t\bar{t}} \sim \sin \alpha / \sin \beta$ ). In practice, however, both situations are disfavored by the combined effect of the unitarity and vacuum stability conditions, together with the flavor physics constraints (mostly from  $B_d^0 - \bar{B}_d^0$ ). Instead, the 2HDM regions with  $\lambda_{hH^+H^-} \sim \mathcal{O}(10^2)$  GeV give rise to

a trademark suppression of the single Higgs boson rates, and pull the relative  $h\gamma\gamma$  coupling strength down to values of  $r \sim -50\%$ . Away from these largely subdued domains, we retrieve total cross sections in the ballpark of  $\langle \sigma_{\gamma\gamma \rightarrow h} \rangle \sim 1 - 50$  fb – this is to say, up to a few thousand neutral,  $CP$ -even, single Higgs boson events, for the light ( $h^0$ ) and the heavy ( $H^0$ ) states alike. Finally, if the Higgs self-interactions are even weaker – or, alternatively, the charged Higgs bosons are very massive – then the  $H^\pm$ -mediated corrections become subleading. In such instances we are left with  $r \lesssim 1$ , as a reflect of the fact that the  $g_{\gamma\gamma h}$  coupling is now essentially determined by a SM-like combination of  $W^\pm$  and fermion-mediated loops. It is also worth underlining the complementary nature of the production rates for the two neutral  $CP$ -even Higgs channels  $\gamma\gamma \rightarrow h^0/H^0$ , which ensues from the inverse correlation of the respective couplings to the charged Higgs, namely of  $\lambda_{h^0 H^+ H^-}$  with respect to  $\lambda_{H^0 H^+ H^-}$  – see the  $\sigma_{h^0}$  and  $\sigma_{H^0}$  curves from panels a-d in Fig. 1. We also observe that the results for  $\gamma\gamma \rightarrow H^0$  tend to be slightly above the SM yields, whereas  $\gamma\gamma \rightarrow h^0$  stays usually below. This follows from the kinematic structure of the total cross section,  $\langle \sigma_{\gamma\gamma \rightarrow h} \rangle \sim M_{M_h}^4/M_W^2$ , which implies  $\sigma_{H^0} > \sigma_{h^0}$  as  $M_{H^0} > M_{h^0} \equiv M_{H_{SM}}$ . In contrast, and owing to its  $CP$ -odd nature,  $\gamma\gamma \rightarrow A^0$  is essentially featureless and entails a minor numerical impact.

### 2.3 Profiling $\gamma\gamma \rightarrow h$ within the MSSM

Let us now turn our attention to the MSSM. On the right panels of Figs. 1-2 we survey the behavior of the purported quantities  $\langle \sigma_{\gamma\gamma \rightarrow h} \rangle$  and  $r$  for the representative MSSM parameter setups that are quoted below [17]:

	$M_{A^0}$ [GeV]	$M_{SUSY}$ [GeV]	$\mu$ [GeV]	$X_t \equiv A_t - \mu/\tan\beta$ [GeV]	$M_2$ [GeV]	$M_3$ [GeV]
no-mixing	400	2000	200	0	200	1600
small $\alpha_e f f$	300	800	2000	-1100	500	500

We note that GUT relations between  $M_1$  and  $M_2$ , as well as universal trilinear couplings ( $A_t = A_b = A_\tau$ ), are assumed throughout. Likewise, we duly account for the impact of the different sets of constraints, most significantly stemming from  $\mathcal{B}(b \rightarrow s\gamma)$  (dashed areas, in yellow) and the Higgs boson and squark mass bounds settled by direct exclusion limits.

In this SUSY setup, non-standard contributions to the effective  $g_{h\gamma\gamma}$  interaction may emerge from a twofold origin. On the one hand we have a panoply of the 2HDM one-loop diagrams mediated by the interchange of virtual charged Higgs bosons. In the present framework, however, these terms do no longer bear any enhancement capabilities, since the corresponding Higgs self-interactions are completely tied to the gauge couplings – as a consequence of the underlying SUSY invariance. On the other hand we find the squark-mediated quantum corrections. Their imprints on  $g_{\gamma\gamma h}$  are mostly visible for relatively light squarks (with masses of few hundred GeV), hand in hand with sizable mass splittings between their respective left and right-handed components and large trilinear couplings to the Higgs bosons <sup>4</sup>. In prac-

<sup>4</sup>The phenomenological implications of this kind of Yukawa, and Yukawa-like couplings have been addressed

tice, however, the combination of the different experimental restrictions effectively tames the abovementioned enlargement power.

We can thus conclude that realistic MSSM scenarios encompass rather mild departures from the SM loop-induced mechanism ( $r \sim -5\%$ ), rendering overall production rates again in the ballpark of  $\langle \sigma_{\gamma\gamma \rightarrow h} \rangle \sim \mathcal{O}(10)$  fb for the lightest  $CP$ -even state  $h = h^0$  while its heavier companions  $H^0, A^0$  lie typically one order of magnitude below [14].

### 3 Discussion and concluding remarks

In this contribution we have reported on the single Higgs boson production through  $\gamma\gamma$  scattering in a TeV-range linear collider. The process  $\gamma\gamma \rightarrow h$  is driven by an effective, loop-induced  $h\gamma\gamma$  interaction, a mechanism that is directly sensitive to the eventual presence of new charged degrees of freedom. We have computed the total cross section,  $\langle \sigma_{\gamma\gamma \rightarrow h} \rangle$ , alongside with the effective (normalized) coupling strength  $r \equiv g_{\gamma\gamma h}/g_{\gamma\gamma H_{SM}}$ , within both the 2HDM and the MSSM. We have disclosed characteristic phenomenological profiles and spelt out their main differences, which mostly stem from the respective Higgs self-interaction structures. In the MSSM, the aforementioned self-couplings are anchored by the gauge symmetry, while in the 2HDM they can be as large as permitted by the combined set of experimental and theoretical restrictions – most significantly unitarity. We have identified a sizable depletion of  $\langle \sigma_{\gamma\gamma \rightarrow h} \rangle$  (corresponding to values of  $r \sim -50\%$ ) for those 2HDM configurations in which a relatively large  $\lambda_{hH^+H^-}$  interaction is capable to thrust the  $H^\pm$ -mediated contribution to  $g_{\gamma\gamma h}$ , and subsequently to maximize the destructive interference that operates between the different  $H^\pm$ ,  $W^\pm$  and fermion-mediated loops. A smoking gun of underlying 2HDM physics would thus manifest here as a missing number of single Higgs boson events. On the MSSM side, departures from the SM are comparably much tempered ( $r \simeq -5\%$ ) and essentially driven by the squark-mediated corrections, which are relatively suppressed by the mass scale of the exchanged SUSY particles and further weakened by the stringent experimental bounds. An additional distinctive feature of both models might manifest from the simultaneous observation of  $\gamma\gamma \rightarrow h^0$  and  $\gamma\gamma \rightarrow H^0$ . Situations where both channels yield  $\mathcal{O}(10^3)$  events per  $500 \text{ fb}^{-1}$  could only be attributed to a non-standard, non-SUSY Higgs sector, since the mass splitting between the two neutral,  $CP$ -even Higgs states is typically enforced to be larger in the MSSM – so that the corresponding  $\gamma\gamma \rightarrow H^0$  rates are comparably smaller.

The clean environment of a linac offers excellent prospects for the tagging and identification of the single Higgs boson final states through the corresponding decay products. The latter should arise in the form of either i) highly energetic, back-to-back heavy-quark dijets ( $h \rightarrow jj$ , with  $jj \equiv c\bar{c}, b\bar{b}$ ); ii) lepton tracks from gauge boson decays ( $h \rightarrow W^+W^- \rightarrow 2l + \cancel{E}_T, Z^0Z^0 \rightarrow 4l$ ); iii) in the specific case of the MSSM, and if kinematically allowed, also the Higgs decays

---

in the past in a wide variety of processes, see e.g. [27].

into chargino pairs ( $h \rightarrow \tilde{\chi}_1 \tilde{\chi}_2 \rightarrow jj + \cancel{E}_T$ ). Precise Higgs boson mass measurements could then be conducted upon the reconstruction of the dijet – or dilepton – invariant masses and should broaden the present coverage of the LHC. For instance, they would enable to sidestep the so-called “LHC wedge”, namely the  $M_{A^0} \gtrsim 200\text{GeV}$  and  $\tan\beta \sim \mathcal{O}(10)$  domains of the MSSM parameter space [28]. The dominant backgrounds, corresponding to the processes  $\gamma\gamma \rightarrow b\bar{b}/W^+W^-$ , could be handled not only by means of standard kinematic cuts, but also through a suitable tuning of the photon beam polarization [15].

A future generation of linac machines, and of  $\gamma\gamma$  facilities in particular, should therefore be instrumental for a precise experimental reconstruction of the EWSB mechanism; namely for the measurement of the Higgs boson mass, couplings and quantum numbers, if not for the discovery of the Higgs boson itself – if its mass and/or its coupling pattern fell beyond the reach of the LHC and the  $e^+e^-$  colliders. Photon-photon physics may well furnish a most fruitful arena in which to carry the Higgs boson research program to completion.

**Acknowledgements** It is a pleasure to thank Joan Solà for the fruitful and enduring collaboration over the past years. I would also like to express my gratitude to the organizers of the LC 2011 workshop at ETC-Trento for the kind invitation to present this review, and for the kind atmosphere and enlightening time we all shared at the meeting.

## References

- [1] ATLAS Collaboration, ATLAS-CONF-2011-157; CMS Collaboration, CMS-PAS-HIG-11-03.
- [2] J.F. Gunion, H.E. Haber, G.L. Kane, S. Dawson, *The Higgs hunter's guide*, Addison-Wesley, Menlo-Park, 1990; G. C. Branco, P.M. Ferreira, L. Lavoura, M.N. Rebelo, M. Sher, J. P. Silva, *Theory and phenomenology of two-Higgs-doublet models*, arXiv:1106.0034.
- [3] M. Moretti, F. Piccinini, R. Pittau, J. Rathsmann, JHEP 1011 (097) 2010, M. Aoki et al, arXiv:1104.3178; G. Bhattacharyya, P. Leser, H. Pas, *Phys. Rev.* **D83** (2011) 011701; S. Chang, J. A. Evans, M. A. Luty, *Phys. Rev. D* **84** (2011) 095030
- [4] H.P Nilles, *Phys. Rept.* **110** (1984) 1; H.E. Haber, G.L. Kane, *Phys. Rept.* **117** (1985) 75; S. Ferrara, ed., *Supersymmetry*, vol. 1-2 (North Holland, World Scientific, 1987).
- [5] D. López-Val, J. Solà, *Phys. Rev.* **D81** (2010) 033003; *Fortsch. Phys.* **G58** (2010) 660; PoS RADCOR2009, 045 (2010).
- [6] *ILC Reference Design Report Volume 2: Physics at the ILC*, arXiv:0709.1893; G. Weiglein et al., *Physics interplay of the LHC and the ILC.*, *Phys. Rept.* **426** (2006) 47, hep-ph/0410364.

- [7] G. Ferrera, J. Guasch, D. López-Val, J. Solà, *Phys. Lett.* **B659** (2008) 297; PoS **RADCOR2007**, 043 (2007), arXiv:0801.3907.
- [8] R. N. Hodgkinson, D. López-Val, J. Solà, *Phys. Lett.* **B673** (2009) 47.
- [9] A. Arhrib, G. Moultaka, *Nucl. Phys.* **B558** (1999) 3; A. Arhrib, M. Capdequi Peyranère, W. Hollik, G. Moultaka, *Nucl. Phys.* **B581** (2000) 34; J. Guasch, W. Hollik, A. Kraft, *Nucl. Phys.* **B596** (2001) 66.
- [10] D. López-Val, J. Solà, N. Bernal, *Phys. Rev.* **D81** (2010) 113005; D. López-Val, J. Solà, PoS **RADCOR2009**, 045 (2010); Fortsch. Phys. 58 (2010) 660.
- [11] See e.g. P. Chankowski, S. Pokorski, J. Rosiek, *Nucl. Phys.* **B423** (1994) 437; V. Driesen, W. Hollik, *Zeitsch. f. Physik* **C68** (1995) 485; A. Djouadi, H.E. Haber, P.M. Zerwas, *Phys. Lett.* **B375** (2003) 1996; A. Djouadi, W. Kilian, M. Mühlleitner, P. M. Zerwas, *Eur. Phys. J* **C10** (1999) 27; S. Heinemeyer, W. Hollik, J. Rosiek and G. Weiglein, *Int. J. of Mod. Phys.* **19** (2001) 535; H. E. Logan, S.-f. Su, *Phys. Rev.* **D66** (2003) 035001; E. Coniavitis, A. Ferrari, *Phys. Rev.* **D75** (2007) 015004; O. Brein, T. Hahn, *Eur. Phys. J* **C52** (2007) 397.
- [12] D. L. Borden, D. A. Bauer, D. O. Caldwell, *Phys. Rev. D* **48**, 4018 (1993); P. Niezurawski, A. F. Żarnecki, M. Krawczyk, *Acta Phys. Polon. B* **34**, 177 (2003)
- [13] N. Bernal, D. López-Val, J. Solà, *Phys. Lett.* **B677** (2009) 38.
- [14] D. López-Val, J. Solà, *Phys. Lett.* **B702** (2011) 246; J. Solà, D. López-Val, *Nuovo Cim.* **C34** (2011) 57.
- [15] B. Grzadkowski, J.F. Gunion, *Phys. Lett.* **B294** (1992) 361; J. F. Gunion, H.E. Haber, *Phys. Rev.* **D48** (1993) 5; S-h. Zhu, C-s. Li, C-s. Gao, *Chin. Phys. Lett.* 15 (1998) 2; M. Mühlleitner, M. Krämer, M. Spira, P. Zerwas, *Phys. Lett.* **B508** (2001) 311; D. M. Asner, J. B. Gronberg, J.F. Gunion, *Phys. Rev.* **D67** (2003) 035009; M. Krawczyk, hep-ph/0307314; P. Niezurawski, A.F. Żarnecki, M. Krawczyk, *Acta Phys. Polon. B* 37 (2006) 1187.
- [16] see e.g. F. Cornet and W. Hollik, *Phys. Lett.* **B669** (2008) 58; E. Asakawa, D. Harada, S. Kanemura, Y. Okada and K. Tsumura, *Phys. Lett.* **B672** (2009) 354; A. Arhrib, R. Benbrik, C.-H. Chen, R. Santos, *Phys. Rev.* **D80** (2009) 015010; E. Asakawa, D. Harada, S. Kanemura, Y. Okada, K. Tsumura, *Phys. Rev.* **D82** (2010) 115002.
- [17] M. Carena, S. Heinemeyer, C. Wagner, *Eur. Phys. J* **C26** (2003) 601.



- [18] T. Hahn, *Comput. Phys. Commun.* **140**, 418 (2001); T. Hahn, C. Schappacher, *Com. Phys. Comm.* **G143** (2002) 54; T. Hahn and M. Pérez-Victoria, *Com. Phys. Comm.* **G118** (1999) 153.
- [19] A. Wahab El Kaffas, P. Osland, O. M. Greid, *Phys. Rev.* **D76** (2007) 095001; H. Flächer, M. Goebel, J. Haller, A. Höcker, K. Mönig, J. Stelzer, *Eur. Phys. J* **C60** (2009) 543; N. Mahmoudi, O. Stål, *Phys. Rev.* **D81** (2010) 035016; S. R. Juárez, D. Morales, P. Kielanowski, arXiv:1201.1876
- [20] F. Mahmoudi, <http://superiso.in2p3.fr>; F. Mahmoudi, *Comput. Phys. Commun.* **178** (2008) 745; *Comput. Phys. Commun.* **180** (2009) 1579.
- [21] S. Kanemura, T. Kubota and E. Takasugi, *Phys. Lett.* **B313** (1993) 155; A. Akeroyd, A. Arhrib, E.-M. Naimi, *Phys. Lett.* **B490** (2000) 119. See also Sect. III of Ref. [5].
- [22] M. Sher, *Phys. Rept.* **179** (1989) 273; S. Nie and M. Sher, *Phys. Lett.* **B449** (1999) 89; S. Kanemura, T. Kasai, Y. Okada, *Phys. Lett.* **B471** (1999) 182; P.M. Ferreira, D.R.T. Jones, *JHEP* 08 (2009) 069.
- [23] D. Eriksson, J. Rathsman, O. Stål, *Com. Phys. Comm.* **G181** (2010) 189, <http://www.isv.uu.se/thep/MC/2HDMC/>.
- [24] P. Bechtle, O. Brein, S. Heinemeyer, G. Weiglein, K. E. Williams, *Com. Phys. Comm.* **G181** (2010) 138; arXiv:1102.1898, <http://www.ippp.dur.ac.uk/HiggsBounds>.
- [25] V. I. Telnov, *Acta Phys. Polon.* **B 37** (2006) 633; A. F. Żarnecki, *Acta Phys. Polon.* **B34** (2003) 2741.
- [26] S. Heinemeyer, W. Hollik and G. Weiglein, *Com. Phys. Comm.* **G124** (2000) 76; S. Heinemeyer, W. Hollik and G. Weiglein, *Eur. Phys. J* **C9** (1999) 343; G. Degrandi, S. Heinemeyer, W. Hollik, P. Slavich, *Eur. Phys. J* **C28** (2003) 133; M. Frank et al., *JHEP* 02 ((2007)) 047.
- [27] J.A. Coarasa, D. Garcia, J. Guasch, R.A. Jiménez, J. Solà, *Eur. Phys. J* **C2** (1998) 373; *Phys. Lett.* **B425** (1998) 329; D. Garcia, W. Hollik, R.A. Jiménez, J. Solà, *Nucl. Phys.* **B427** (1994) 53; S. Béjar, J. Guasch, D. López-Val, J. Solà, *Phys. Lett.* **B668** (2008) 364.
- [28] H. Haber, *J. Phys. Conf. Ser.* **G259** (2010) 012017.